IOPscience iopscience.iop.org

Home Search Collections Journals About Contact us My IOPscience

Experimental study of reversed shear Alfvén eigenmodes during the current ramp in the Alcator C-Mod tokamak

This content has been downloaded from IOPscience. Please scroll down to see the full text.

2010 Plasma Phys. Control. Fusion 52 115003

(http://iopscience.iop.org/0741-3335/52/11/115003)

View the table of contents for this issue, or go to the journal homepage for more

Download details:

IP Address: 198.125.176.142
This content was downloaded on 07/03/2016 at 18:31

Please note that terms and conditions apply.

Plasma Phys. Control. Fusion **52** (2010) 115003 (15pp) doi:10.1088/0741-3335/52/11/115003

Experimental study of reversed shear Alfvén eigenmodes during the current ramp in the Alcator C-Mod tokamak

E M Edlund[1], M Porkolab[2], G J Kramer[1], L Lin[3], Y Lin[2], N Tsujii[2] and S J Wukitch[2]

[1] Princeton Plasma Physics Laboratory, Princeton, NJ 08543, USA
[2] MIT Plasma Science and Fusion Center, Cambridge, MA 02139, USA
[3] University of California Los Angeles, Los Angeles, CA 90095, USA

E-mail: eedlund@pppl.gov

Received 4 May 2010, in final form 29 July 2010
Published 27 September 2010
Online at stacks.iop.org/PPCF/52/115003

Abstract
Experiments conducted in the Alcator C-Mod tokamak have explored the physics of reversed shear Alfvén eigenmodes (RSAEs) during the current ramp. The frequency evolution of the RSAEs during the current ramp provides a constraint on the evolution of $q_{\min}$, a result which is important in transport modeling and for comparison with other diagnostics which directly measure the magnetic field line structure. Additionally, a scaling of the RSAE minimum frequency with the sound speed is used to derive bounds on the adiabatic index, a measure of the plasma compressibility. This scaling places the adiabatic index at 1.40 ± 0.15 and supports the kinetic calculation of separate electron and ion compressibilities with an ion adiabatic index close to $7/4$.

(Some figures in this article are in colour only in the electronic version)

1. Introduction

Magnetized plasmas covering many orders of magnitude in size, from earth-bound devices such as the tokamak [1], to planetary aurora [2] and stellar systems [3] exhibit a type of electromagnetic oscillation known as the shear Alfvén wave [4]. In tokamaks, shear Alfvén waves can be destabilized by the radial gradient of the energetic ion pressure [1], which may arise from ion-cyclotron resonance heating (ICRH) [5], neutral beam heating [6] or fusion-born alphas [7]. Shear Alfvén waves have the potential to enhance the loss of energetic ions through resonant transport [8, 9], an important consideration for future burning plasma experiments. As a contribution to this larger field of transport studies, we comment here on a particular class of shear Alfvén waves known as the reversed shear Alfvén eigenmode (RSAE, also Alfvén cascade) and may be excited in tokamak plasmas during the current ramp

 © 2010 IOP Publishing Ltd Printed in the UK & the USA

[10–12] or during sawteeth [13, 14]. The RSAE is unique among the larger class of Alfvén eigenmodes in that it is particularly sensitive to small changes in $q_{\min}$, that is the minimum of the function $q(r) \approx rB_\phi/R_0B_\theta$. The inversion of the RSAE frequency spectra as a method for inferring particular plasma properties, such as $q_{\min}$, is known as 'MHD spectroscopy' [15] and is the focus of this paper. We approach this problem through the comparison of local measurements of RSAEs with a thermodynamic analysis of Alfvén waves, a kinetic treatment of RSAEs and an established ideal MHD code which calculates the Alfvén wave structure and frequency in toroidal geometry to derive measures of the adiabatic index (γ) and the evolution of $q_{\min}$ during the current ramp. A well-constrained account of the current diffusion process, through the parameter q, provides a useful constraint for transport modeling or comparison with direct measurements of the magnetic field structure, as from the motional Stark effect (MSE) diagnostic. A measure of the plasma adiabatic index provides a simple way to compare predictions from thermodynamic, MHD and kinetic models.

The dispersion relation of the ideal shear Alfvén wave is $\omega_A = k_\parallel v_A$, where $k_\parallel = (\vec{k}\cdot\vec{B})/B$ is the wavenumber parallel to the equilibrium magnetic field, $v_A = B/(\mu_0\rho)^{1/2}$ is the Alfvén speed and ρ is the mass density. In toroidal geometry the magnetic field line curvature, arising from a combination of the toroidal component which scales as $1/R$ and the poloidal component due to the plasma current, allows very weakly damped Alfvén waves to exist as eigenmodes of the system with discrete frequencies [16]. The magnetic safety factor (q) describes the winding of the magnetic field lines and is an important parameter in the study of Alfvén eigenmodes in toroidal geometry. A particular class of eigenmode, the RSAE, exists when the q profile exhibits an off-axis minimum[4]. A minimum in q, hereafter $q_{\min}$, exists transiently during the initial current ramp phase of tokamak operation when the Ohmic current density has an off-axis peak and diffuses toward the plasma core.

In axisymmetric devices such as the tokamak, the toroidal mode number (n) unambiguously identifies a normal mode of oscillation on account of the absence of the azimuthal coordinate in the equations of motion. In contrast, effects such as the $1/R$ variation of the toroidal magnetic field and plasma shaping tend to couple poloidal mode numbers (m), rendering a description in terms of an expansion in poloidal harmonics as an infinite set of coupled equations. However, RSAEs are unique among the larger class of Alfvén eigenmodes in that they are composed of a single dominant poloidal mode which permits a truncation of the equations to the m and $m \pm 1$ components, from which a simple dispersion relationship may be derived [18–21]. RSAEs are characterized by a frequency which starts from a non-zero minimum value and which rises as $q_{\min}$ decreases, reaching a maximum frequency near the TAE (toroidicity-induced Alfvén eigenmode) frequency defined by $\omega_{TAE} = v_A/2qR_0$. When the RSAE frequency is far from the TAE frequency, the dispersion relationship derived from a WKB analysis is of the form [19, 20]

$$\omega_{RSAE}^2 = \omega_{\min}^2 + \omega_A^2 + (\Delta\omega)^2, \tag{1}$$

where ω_A is a function of $k_\parallel$ as defined previously and in toroidal geometry,

$$k_\parallel \approx \frac{n}{R_0}\left(\frac{m}{nq_{\min}} - 1\right). \tag{2}$$

The first term on the rhs of (1) is a function of the local sound speed, equal to $2\gamma(T_e+T_i)/m_iR_0^2$, where T_e and T_i are the electron and ion temperatures, m_i is the ion mass and R_0 is the tokamak major radius. In Alcator C-Mod plasmas this term provides a non-zero minimum frequency of

[4] A noted exception to this case may be found when q is slightly greater than unity, as may occur following a sawtooth crash [13]. More fundamental than a minimum in q, the RSAEs require an extremum in the Alfvén continuum [17]. In the case of $q \gtrsim 1$ the Alfvén continuum retains a local maximum only when q also has a local maximum.

approximately 200 kHz. The second term describes the Alfvénic contribution which can vary between 0 and about 500 kHz. The $(\Delta\omega)^2$ term captures other effects as may arise from kinetic contributions of the energetic ions [19] and represents a perturbation to the frequency. When the Alfvénic term is small, (1) is dominated by the minimum frequency component which allows the unknown parameter γ to be inferred when the frequency and temperatures are known. The Alfvénic term grows as $k_\parallel$ increases due to a change in $q_{\min}$. The quadratic nature of (1) means that when the Alfvénic term is only about 1.5 times the minimum frequency term, the RSAE frequency will grow nearly linearly with $k_\parallel$. This implies that the rate of frequency rise for a given n is approximately proportional to n, which allows the observed spectrum of modes to be uniquely determined even in the absence of direct mode measurement by magnetic pick-up coils. In this paper we present a comparison of spectral measurements of Alfvén waves to theoretical models as a means of inferring $q_{\min}$ and γ. Section 2 presents the experiments and methods by which the RSAEs are studied. Section 3 establishes an experimental basis for the evolution of $q_{\min}$ during the current ramp, an important result for transport modeling. The physics of the minimum frequency of the RSAEs, with special attention to the role of the adiabatic index, is investigated in section 4. The paper closes with concluding remarks in section 5.

2. Experimental conditions and diagnostics

The Alcator C-Mod tokamak is a high-field ($B_\phi < 8$ T), compact tokamak ($R_0 = 0.68$ m, $a = 0.22$ m, $\kappa \leqslant 1.85$), which employs minority ICRH as the main auxiliary heating mechanism. An overview of several important experimental parameters for a representative shot is presented in figure 1. The plasma remained in L-mode during the current ramp phase of these experiments, in a configuration which was limited by the inner wall. For all experiments reported in this paper, the axis magnetic field was set between 5.2 and 5.5 T. The plasmas used a d(h) (deuterium majority, hydrogen minority) mixture with $n_{\rm h}/n_{\rm d} \approx 0.05$. The dominant impurity species tends to be high Z, most likely Mo^{+32} resulting from the all metallic (molybdenum) first wall in Alcator C-Mod [22, 23]. Electron density and temperature profiles are derived from the electron-cyclotron-emission (ECE) and Thomson scattering diagnostics, respectively. Typical electron densities at the magnetic axis are in the range $(1.2\text{–}1.6) \times 10^{20}\,\mathrm{m}^{-3}$. The injected ICRH power was varied over 2–5 MW across the set of experiments, resulting in electron temperatures in the 3–6 keV range. Typical hydrogen ion energies are 100 keV and may have a slightly hollow profile, but is expected to have a decreasing gradient in the region of $r/a = 0.3$ near the peak of the RSAEs [24]. We expect $\tau = T_{\rm i}/T_{\rm e}$ to be less than one in these plasmas, as the energetic protons generated by the ICRH first slow down on electrons which then thermalize with the deuterium majority.

Unlike the electron temperature which is directly measured by the ECE diagnostic, the ion temperature in Alcator C-Mod can only be inferred through a spatially averaged measure of the dd neutron rate. We pause here to briefly discuss the uncertainties in this value and its impact on the inference of γ, the subject of section 4. The neutron emission rate from dd fusion is proportional to $n_{\rm i}^2 T_{\rm i}^{-2/3} \exp(-20.1/T_{\rm i}^{1/3})$ [25], where $T_{\rm i}$ is in keV, averaged over the profile. The exponential dependence of this function results in an approximate $T_{\rm i}^4$ dependence in the temperature range of interest. Inverting this relation to solve for the ion temperature in terms of the neutron rate, we find an approximate $n_{\rm i}^{-1/2}$ dependence. With a $Z_{\rm eff}$ of 4, typical of the current ramp phase, we must consider how the impurities modify the deuterium density relative to the electron density (which is a measured quantity). Assuming a single, high Z impurity species is present, it is straightforward to show that $n_{\rm i}/n_{\rm e} \approx 1-(Z_{\rm eff}-1)/Z_{\rm I}$. Taking

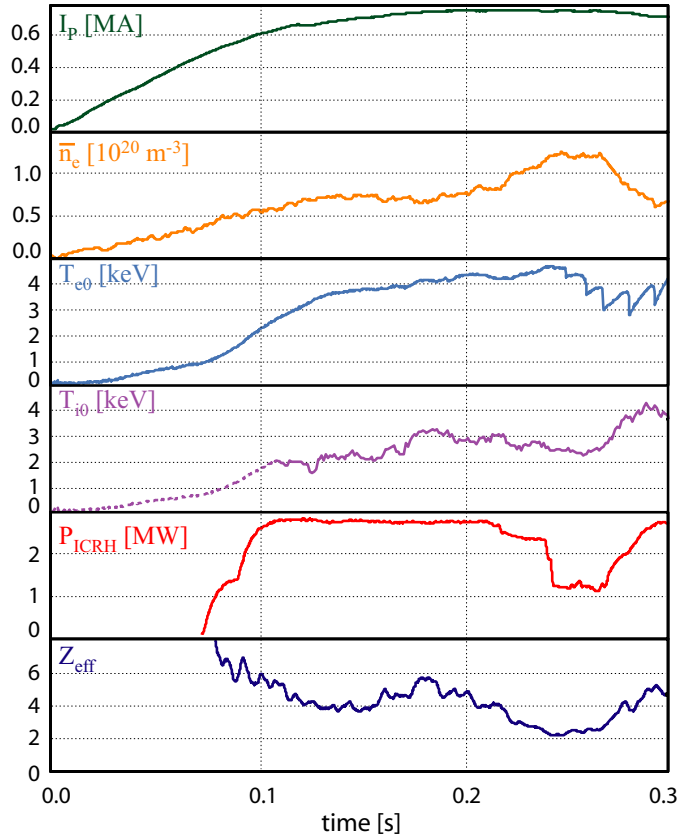

Figure 1. Overview of plasma parameters corresponding to the experiment examined in figure 3. (Color online.)

$Z_I \sim 32$ and $Z_{eff} \sim 4$ gives $n_i/n_e \sim 0.9$, resulting in an increase in the ion temperature by a factor of approximately 1.05. Conversely, the largeness of Z_I means that the impurity density normalized to the electron density is of order 10^{-3}. The ratio of the actual mass density (ρ) to $n_e m_i$ is approximately $1 + (5 - Z_{eff})/2Z_I$ when we consider a deuterium majority and a molybdenum impurity. Again using $Z_{eff} \sim 4$ gives a normalized mass density of approximately 0.98. Given that the thermal speed scales like $\bar{v}_{th} \approx 2(T_e + T_i)^{1/2}/\rho$, the impurity's tendency to increase the measured T_i and decrease the mass density results in a net increase in the thermal speed of about 5% over the impurity-free case when we take $T_i/T_e \sim 0.75$. Without further measurements of the impurity density profile it is impossible to provide a more accurate measure of the ion temperature and density. We therefore conclude that even in the presence of a substantial Z_{eff} we may with reasonable accuracy neglect the impurity species and cite a potential 5% increase in the effective thermal speed. The conclusion regarding the inference of γ from the RSAE frequency measurements is that the value derived assuming no impurities is an upper bound, as follows from the relation $\omega_{min} \sim \gamma^{1/2}\bar{v}_{th}/R_0$.

A central feature of the experiments examined here is the diffusion of the ohmic current from the plasma periphery toward the core. This process occurs on a resistive timescale $\tau_\eta = \mu_0 L^2/\eta$, where η is the plasma resistivity which scales as $T_e^{-3/2}$ [26]. The resistive diffusion time for Alcator C-Mod, taking $T_e \sim 2$ keV as representative of the early part of the

current ramp and using $L \sim a/2$ gives $\tau \sim 200$ ms. Observations of sawteeth oscillations (a periodic internal reconnection event occurring near the $q = 1$ surface) are in good agreement with this scaling, with a typical onset time of about 250 ms. In the experiments reported here, ICRH is injected during the current ramp phase to generate the energetic ions which destabilize the RSAEs and also to increase the temperature as a means of retarding the current penetration.

The phase contrast imaging (PCI) system on Alcator C-Mod [11, 27] is the primary diagnostic used in these experiments. The PCI diagnostic is sensitive to perturbations in the electron density (relative to the background), which, for example, may be induced by shear Alfvén waves. The Alcator C-Mod PCI system uses a 80 W CO_2 laser, which passes vertically through plasma, allowing for detection of perturbations from all flux surfaces. The phase plate, the central optical component of the diagnostic, applies a high pass filter to the wavenumber spectrum with a shoulder of approximately 0.5 cm^{-1}. An image is formed at a 32 element photoconductive HgCdTe detector, allowing for radial resolution of about 3 mm. The image intensity is proportional to the line integral of the electron density perturbations along the beam path, that is, $I_{\mathrm{PCI}} \propto \int \tilde{n}_{\mathrm{e}}\, \mathrm{d}z$, where $\tilde{n}_{\mathrm{e}}$ is the perturbed component of the electron density. This means that the two-dimensional perturbation structure of the mode is compressed into a one-dimensional image. While some information is lost through this process, the output signal captures the line integral of the complex-valued (phase dependent) perturbations and provides a high degree of structure which can be used to compare with code predictions. Measurements of the structure and frequency of the AEs are supported by measurements with the Mirnov coil array, composed of two groups of coils at ± 10 cm from the midplane (figure 2). Measurements of the toroidal phase of the RSAEs by the Mirnov coils supports the identification of mode numbers derived from PCI analysis of the collective spectral features of the RSAEs [13].

3. RSAEs during the current ramp

As noted in the previous section, the timescale for current diffusion during the current ramp is of order 200 ms. At the time of plasma formation a negligible current density exists in the core and q_0, that is q at the magnetic axis, is effectively infinite, with the plasma current localized nearer to the edge. However, the cooler temperatures of the early plasma cause a very rapid penetration of current. An earlier study of RSAEs in Alcator C-Mod found larger values of q_{min} [28] compared with what we report here. While differences in the startup and heating schemes may produce some difference in the current penetration, the results reported here are representative of the majority of experiments where RSAEs are present. Additionally, [28] used the MISHKA code which at the time did not properly account for the offset in the minimum frequency which may have introduced a significant offset in the analysis. A similar but more complete study is reported here using NOVA, which includes coupling to acoustic modes which provides a minimum frequency offset, yielding a more stringent constraint on the evolution of q_{min} during the current ramp. The finding of $q \sim 2$ during the current ramp provides a timescale for the diffusion of current in agreement with the appearance of sawteeth, a factor not considered in the earlier work.

In these experiments, ICRH was injected into the plasma starting at about 80 ms; coupling prior to this time is poor and much of the energy would be reflected. It follows that the period in which RSAEs may be excited by the ICRH-generated energetic ions extends from about 80 ms to about 200 ms when the reversed magnetic shear vanishes, though in practice the active period is reduced at the earlier times by inefficient heating of the cool hydrogen minority. In the intermediate phase we expect q to cross the integer value 2, at which point a so-called 'grand cascade' develops, a spectral structure characterized by multiple RSAEs

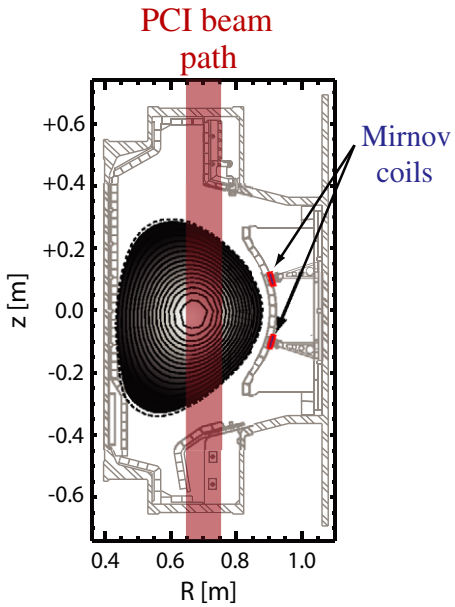

Figure 2. Cross section of the Alcator C-Mod tokamak showing the position of the PCI beam path and the poloidal location of the two sets of Mirnov coils. (Color online.)

originating from the same minimum frequency and chirping in frequency proportional to their individual toroidal mode numbers [10]. A grand cascade provides an excellent benchmark for matching of calculated spectra to observed spectra and is clearly visible in the PCI spectrogram of figure 3(*a*) starting around 130 ms.

Numerical MHD analysis of these experiments was conducted with the ideal MHD code NOVA [29] which employs a non-variational approach to solutions using iteration of the eigenvalue (frequency). NOVA accepts arbitrary density, temperature and q profiles and includes the geometric effects of toroidicity and triangularity. A range of ideal MHD modes including RSAEs, TAEs and EAEs (ellipticity-induced Alfvén eigenmodes), among others, may be studied with NOVA. While it does not perform time-dependent simulations, NOVA can model the evolution of the plasma equilibrium under the quasi-static approximation. This technique is applied in the subsequent analysis to derive the time evolution of $q_{\min}$ during the current ramp phase, which requires simply that the RSAE period be much smaller than the resistive diffusion time, a condition well satisfied since the diffusion time is of order 10^{-1} s while the RSAE period is of order 10^{-5} s. It should be noted that NOVA calculates the eigenmodes from a linearized analysis of the MHD equations, and therefore, is incapable of predicting saturated amplitudes. For this reason, the comparisons between experiment and theory reported here consider only the frequency and spatial structure of the fluctuations.

The q profile given to NOVA is described by a 6th order polynomial which is matched to the edge q profile calculated by EFIT [30]. Three free parameters in the fitted q profile are q_0, $q_{\min}$ and $r_{\min}$, the radial position of the minimum. While these values are initially unknown, it has been shown that comparison of the PCI data with a synthetic PCI analysis based on NOVA calculations is sufficient to constrain $q_{\min}$ and $r_{\min}$ and is relatively insensitive to q_0 [13]. RSAE spectra calculated from over 600 NOVA runs using a q profile which decreases in time are presented in figure 3(*b*). During the period of RSAE activity the q profile decreases at

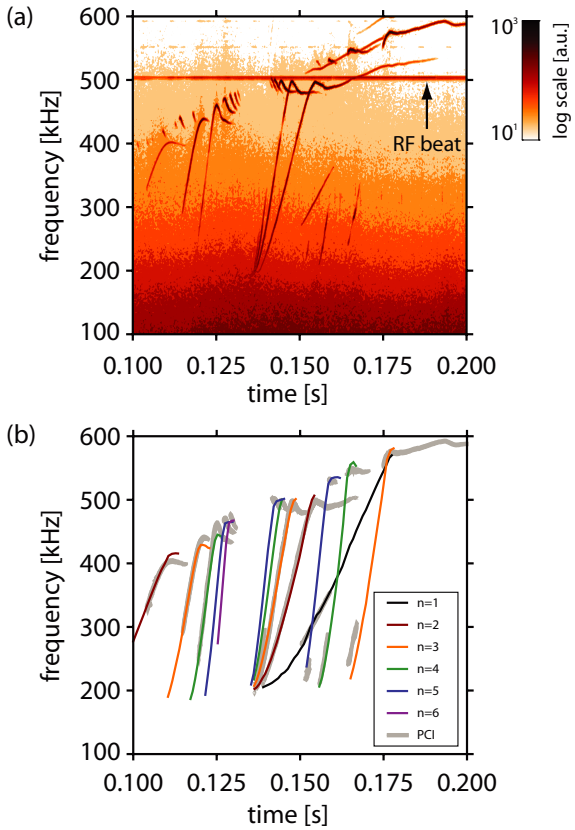

Figure 3. (*a*) Composite spectrogram averaged over all 32 channels of the PCI diagnostic. RSAEs are present during the time range 100–180 ms, with a grand cascade occurring at approximately 130 ms which identifies the entrance of the $q = 2$ surface to the plasma. (*b*) RSAE spectra calculated by NOVA (color) as the q profile is decreased are compared with experimental PCI measurements (gray), allowing the evolution of $q_{\min}$ to be determined. (Color online.)

a nearly constant rate, illustrated in figure 5. Termination of the RSAEs at about 180 ms implies a loss of a reversed shear profile, as the ICRH power coupled to the plasma is steady over this time. The development of the sawtooth oscillation starting around 240 ms implies that $q_{\min}$ is near to unity at that time [13]. The extrapolation of $q_{\min}$ determined by RSAE spectroscopy to that constrained by sawteeth lies between a form described by $\partial_t q =$ constant and $\partial_t \ln q =$ constant. The former describes the evolution of a current which is forced by the external control system, and the latter a case where the current diffuses under the constraint that the total current remains constant. The fact that the evolution lies somewhere between these curves is expected on the grounds that the current ramp ends at about 200 ms, at which time the evolution transitions from driven to free diffusion. Unlike numerical transport models that calculate the current profile evolution, inferences of $q_{\min}(t)$ from MHD spectroscopy has negligible dependence on the plasma impurity content and is a more robust method.

An additional constraint on NOVA calculations is found in the spatial structure of the RSAEs. The diagnostic compression of the two-dimensional structure to a one-dimensional image in the experimental PCI measurements represents a loss of data. To compare the NOVA model results with the measurements, a synthetic diagnostic approach is used, whereby the

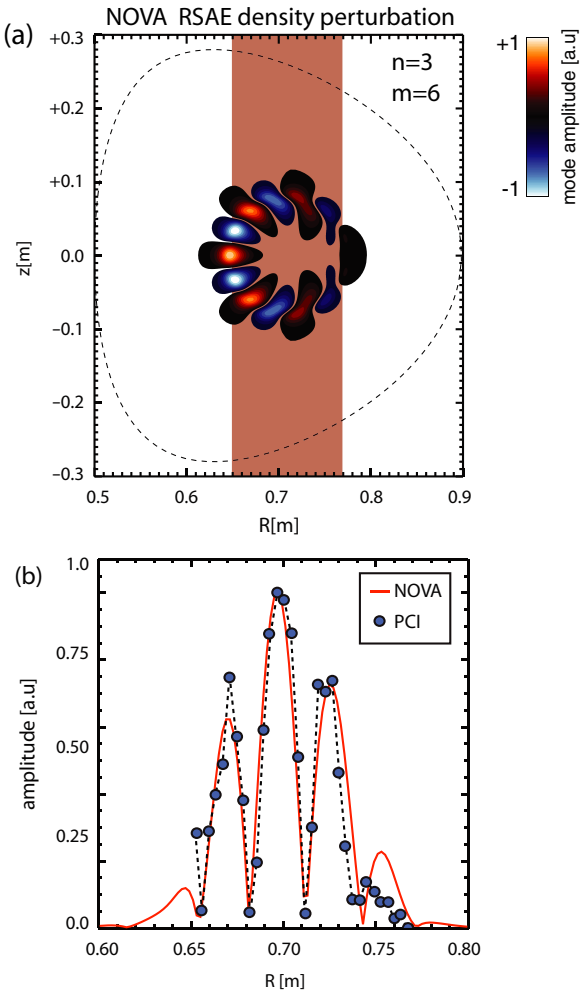

Figure 4. (*a*) The two-dimensional density perturbation calculated by NOVA for the $n = 3$ mode near 140 ms identified in figure 3. The shaded area indicates the PCI viewing region. (*b*) The synthetic PCI data are compared with the experimental data, showing overall good agreement between the structures. The nodes in the structure arise from cancelation of positive and negative density perturbations. (Color online.)

density perturbation is integrated and spatially filtered according to the diagnostic response [13, 31]. A best-fit solution for an $n = 3$ mode is presented in figure 4, where the radial position of $q_{\min}$ was found to be $r_{\min}/a \approx 0.30 \pm 0.05$. The nodes in the radial structure arise due to cancelation of signal from summation over positive and negative density perturbations and are particularly sensitive to variations in $r_{\min}$. At this time, we have been unable to identify a robust experimental constraint for the value of q_0 and this parameter remains largely unknown through these methods, which also means that this parameter does not significantly affect the analysis of the other two free parameters, $q_{\min}$ and $r_{\min}$.

This analysis offers an account of the evolution of q during a current ramp representative of startup in Alcator C-Mod with early ICRH. These results may find application in modeling transport during the current ramp or in validating future diagnostics which provide a more

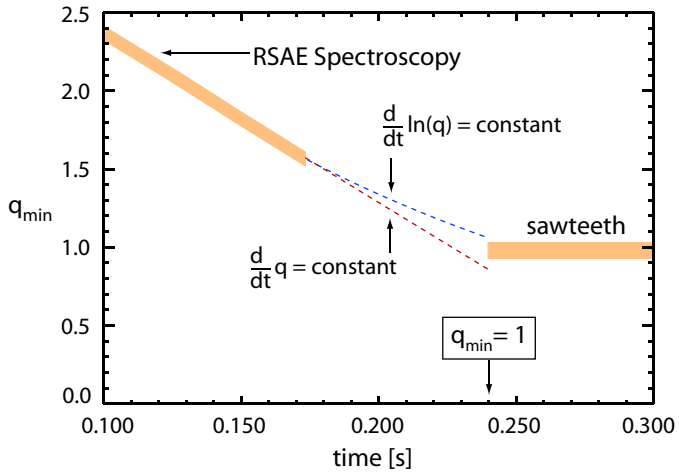

Figure 5. MHD spectroscopy of the RSAEs (100–180 ms) and the presence of sawteeth (240+ ms) provide limits for the evolution of $q_{\min}$ during the current ramp. Extrapolation of the inferred $q_{\min}$ trajectory to the time of sawteeth is seen to lie between the curves $\mathrm{d}_t q = \text{constant}$ and $\mathrm{d}_t \ln q = \text{constant}$. (Color online.)

direct measure of the magnetic structure. Although NOVA successfully produces solutions which described the evolution of the RSAEs in the Alfvénic regime (the linear chirp regime), it struggles to find proper solutions when the frequency is near the minimum frequency. Special care must be taken to analyze this regime, the focus of the next section.

4. RSAE minimum frequency

Theoretical analysis of RSAEs has shown that the finite minimum frequency is due to a deformation of the Alfvén continuum by coupling to geodesic acoustic waves [19, 20, 32, 33]. In the absence of this coupling the Alfvén continuum would vanish when $q = m/n$ giving $\omega_{\min} = 0$, whereas with coupling the continuum is lifted to a minimum frequency which to first order is proportional to the local sound speed. In the MHD model employed in NOVA the sound speed takes the form $(\gamma p/\rho)^{1/2}$, where γ is the adiabatic index of the plasma, p is the total thermal pressure and $\rho = n_{\mathrm{e}} m_{\mathrm{i}}$ is the mass density. Thus, simultaneous measurement of the RSAE minimum frequency with T_{e} and T_{i} provides a means by which the adiabatic index can be inferred. Finite pressure effects enter the linearized perturbation equations in NOVA through an equation of state of the form $\mathrm{D_t}(\mathrm{p}/\rho^{\gamma}) = 0$. An adiabatic index of $5/3$ may be used when the plasma can be treated as an ideal gas, a condition valid when the magnetic perturbations are sufficiently weak that they do not contribute to the force and energy balance, but is not a situation generally applicable to a strongly magnetized plasma. While ideal MHD theory allows for an arbitrary value of γ, additional information is needed to predict what value should be used. We present here an argument that, at least when considering Alfvén eigenmodes, a significantly lower value of γ should be used to properly model compressional effects.

In a single fluid model, the adiabatic index can be related to the thermodynamic relation between the pressure and internal energy of gas. The work of McKee and Zweibel [34] provides a compelling argument that γ should be close to the value $3/2$ for shear Alfvén waves. In the ideal limit, shear Alfvén waves scan be represented as a coupling of fluid and

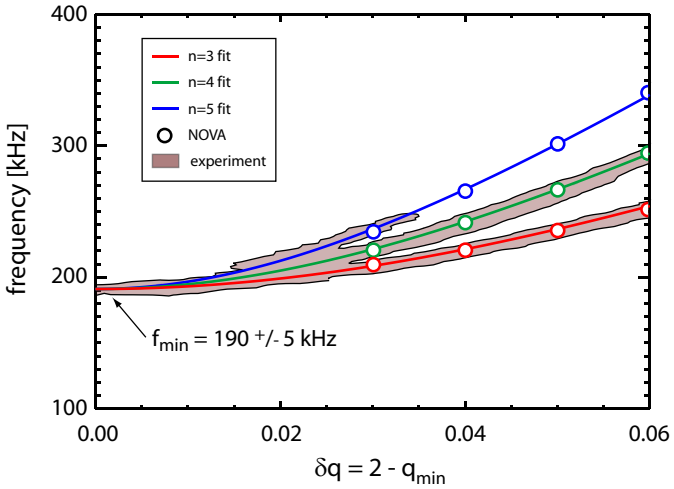

Figure 6. While NOVA cannot directly calculate $f_{\min}$ on account of the larger continuum interaction which distorts the eigenmodes, it can produce viable solutions in the neighborhood of $f_{\min}$. Using an analytic approximation (colored lines) the NOVA frequencies (circles) are extrapolated to a common minimum frequency, which agrees well with the experimental measurements of the minimum frequency (shaded region). (Color online.)

magnetic perturbations of the form $v_1 = v_A B_1/B_0$, where a subscript '1' refers to a first order perturbation. While the total energy of the shear Alfvén wave increases due to the magnetic contributions, the pressure, on the other hand, decreases due to the restoring force supplied by the magnetic fields. Hence, the definition of γ through the thermodynamic relation between pressure and energy, $p = (\gamma - 1)U$, dictates that $\gamma = 3/2$ when the equations of motion are substituted. The Alfvén eigenmodes realized in experiment are not true shear Alfvén waves as they necessarily contain a compressional component, an effect which can be quite important for proper interpretation of the measured mode structures [35].

While NOVA produces viable RSAE solutions in the Alfvénic regime, their structure when ω_{RSAE} is close to $\omega_{\min}$ is not well resolved. Inclusion of higher order terms (finite Larmor radius corrections), not present in the NOVA model, resolves this ambiguity [36]. However, a minimum frequency can yet be derived from the NOVA analysis by using an analytic dispersion relation which is a good approximation to the general form of the solutions, in conjunction with the good solutions from NOVA which are found slightly away from the minimum. The dispersion relation given in (1) provides two important features which are used to determine NOVA's minimum frequency: the quadratic form with respect to the parameter $\delta q = m/n - q_{\min}$ and the divergence of the separate RSAE spectral lines as δq increases from zero. This model allows extrapolation of the frequencies calculated by NOVA to the common minimum frequency, as illustrated in figure 6. Motivated by the work of Breizman *et al* [19], where finite pressure effects were included, we have explored the dependence of the NOVA model on profile gradients. To isolate the gradient dependence from the magnitude dependence, the temperature and density were held fixed at a radius of $r/a = 0.3$ (the same radial position as $q_{\min}$) while the gradients were scanned by changing the profile shape. Figure 7 presents the summary of the profile scan, showing that the temperature and its gradient determine the minimum frequency and that the density does not play a role, as was expected from theory. While ideal MHD does not explicitly involve the temperature in any of its equations, the ratio of the pressure to the density does enter and provides an effective mean temperature by which

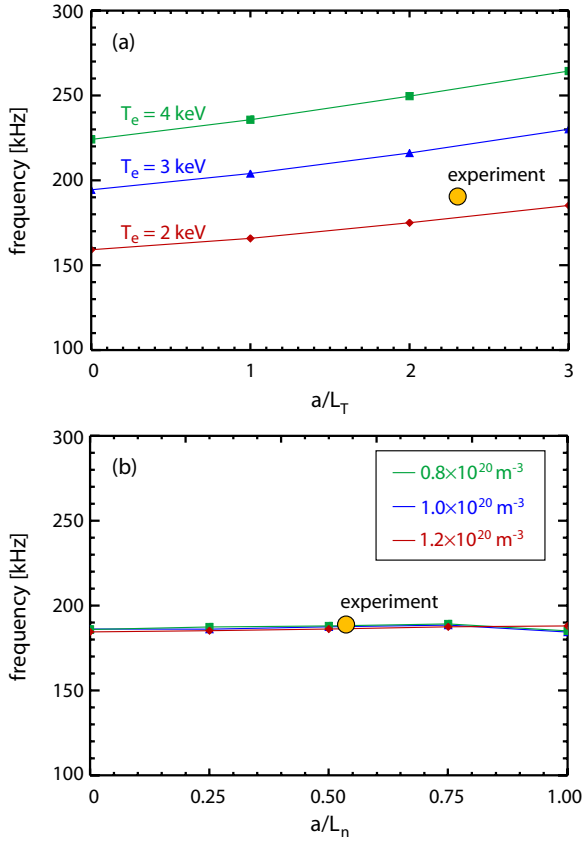

Figure 7. Parameter scans in NOVA show that the minimum RSAE frequency has (*a*) a strong temperature dependence and weaker temperature gradient dependence and (*b*) no significant dependence on density and density gradient. The gradient scans were performed with the value of the profile held constant at the peak of the eigenmode. For the experimental data shown in figure 6 the electron temperature near $q_{\min}$ is about 2.3 keV, in good agreement with an interpolation of the scaling studies shown here. (Color online.)

the described minimum frequency dependence arises. These studies allowed an empirical dispersion relation for the RSAE minimum frequency in terms of the temperature and its gradient to be derived, given here as

$$\omega_{\mathrm{NOVA}} = 100 T_{\mathrm{e}}^{1/2} \sqrt{\gamma + 0.15 \frac{r}{L_T}}, \tag{3}$$

where T_{e} is in keV, r is the radius of the peak of the RSAE and $L_T^{-1} = -\mathrm{d}\ln(T_{\mathrm{e}})/\mathrm{d}r$ is the temperature gradient scale length. We may compare this empirical relation with the collection of experimental data of minimum frequency measurements and minimize the difference to derive a best fit γ. This analysis is illustrated in figure 8, and indicates that $\gamma = 1.40 \pm 0.15$. The vertical error bars on the data points represent the uncertainty in the resolution of the minimum frequency determined by experiment, while the limits of γ at 1.25 and 1.55 arise from uncertainty in the temperature profiles and enter through the empirical dispersion relation of (3). The exclusion of $\gamma = 5/3$, the ideal gas value of the adiabatic index, indicates that additional physics beyond that of free particles is present in the energy and pressure balance

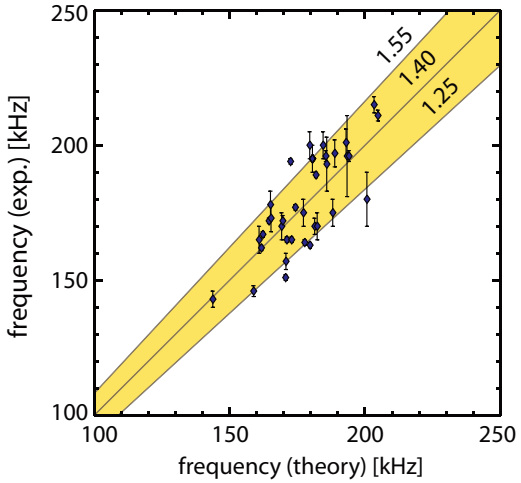

Figure 8. The collection of minimum frequency data is compared with the empirical NOVA scaling of the minimum frequency to derive γ. This analysis finds a best fit γ of 1.40 ± 0.15, with the error bars resulting from the uncertainties in the experimental temperature profiles.

of these waves, a result which is not surprising given that these waves necessarily involve a perturbation of the magnetic field.

In the plasmas of interest the electron thermal velocity may be twice the parallel phase velocity of the RSAEs. The largeness of the electron thermal velocity implies that the adiabatic index of the electrons is equal to 1 in a two-fluid analysis whereas the ions are described by an adiabatic index of γ_i, calculated to have the value 7/4 [33, 37]. We have compared the minimum frequency data from the RSAEs with the kinetic treatment of RSAEs by Breizman *et al* [19] which provides the following form for the minimum frequency,

$$\omega_{\mathrm{min}}^2 \approx \frac{2T_\mathrm{e}}{m_\mathrm{i} R_0^2}(1 + \gamma_\mathrm{i}\tau), \tag{4}$$

where γ_i is given as 7/4. As this form does not include any free parameters, we make a comparison with this general form letting the ion adiabatic index (γ_i) be a free parameter and adjust this value until a best fit to the RSAE minimum frequency data is found. This study is summarized in figure 9, showing a best-fit value of $\gamma_\mathrm{i} \approx 1.8$, a value very close to the predicted 7/4. We may relate the kinetic treatment to the former MHD treatment through an effective adiabatic (γ_eff) which captures the electron and ion response by equating the sound speeds,

$$\gamma_\mathrm{eff} = \frac{1 + \gamma_\mathrm{i}\tau}{1 + \tau}. \tag{5}$$

We note that γ_eff is only a function of the ion to electron temperature ratio (τ) and ranges from 1.33 to 1.4 over the range $\tau = 0.70$ to 1.0 for $\gamma_\mathrm{i} = 1.8$, in reasonable agreement with the values derived by the MHD analysis. It should be noted that this form is not a precise definition, as the γ derived from the MHD analysis included effects of temperature gradients which are not represented here. We conclude from this analysis that the three models considered here (thermodynamic, MHD, kinetic) are all roughly in agreement when the energy and pressure of the Alfvén waves are accounted for.

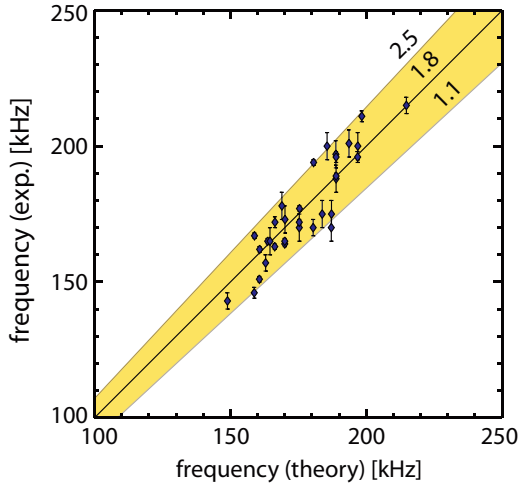

Figure 9. The collection of minimum frequency data is compared with 4. The analysis finds a best-fit value of the *ion* adiabatic index (γ_i) of approximately 1.8, a result very close to the theoretical prediction of 7/4.

5. Summary and conclusions

Two primary results are reported in this paper. The first is that comparison of the RSAE frequency spectra observed during the current ramp phase of Alcator C-Mod experiments to numerical results from the ideal MHD code NOVA provide a method by which the evolution of the q profile may be constrained. In the absence of other diagnostics which provide direct measurements of the magnetic field structure, these observations represent the only constraints on the central q profile which are independent of a current diffusion model. In addition to the evolution of $q_{\min}$, comparison of the one-dimensional spatial structure measured by the PCI diagnostic to a synthetic PCI analysis of NOVA data shows that the radial position of $q_{\min}$ may also be determined. Current diffusion calculations from TRANSP may be compared against these measurements to determine what particular models are best suited for the current ramp phase. A measurement on the current profile evolution is an important constraint for use with transport codes which calculate the Ohmic heating profiles.

In addition to the MHD spectroscopic results of the Alfvénic regime, analysis of the minimum frequency scaling with T_e is a method by which the plasma adiabatic index can be inferred. While the MHD model may be criticized for using a simplified equation of state, the ubiquity of MHD codes and their proven utility motivates a desire to constrain the remaining free parameters in the model. Little attention has been paid to the adiabatic index, a parameter which is difficult to measure but which has important consequences for the MHD spectroscopy [35] and possibly mode stability. Comparison of a set of minimum frequency measurements of RSAE spectra by the PCI diagnostic reveals a best-fit γ in the neighborhood of 1.40 ± 0.15, close to the ideal limit of 3/2 predicted theoretically from thermodynamic arguments [34]. The adiabatic index derived by this method is representative of magnetic and fluid perturbations particular to shear Alfvén waves, and it should be cautioned that other plasma waves may express an adiabatic response different from that determined here. A comparison of the same minimum frequency data to a kinetic analysis of RSAEs [19] finds good agreement with the theoretically derived ion adiabatic index value of 7/4. As a final note we would like to mention possible extensions of this work to account for additional kinetic

effects of energetic ions. The theoretical treatment of the energetic ion influence on the RSAE dispersion relation by Breizman *et al* [19] has shown that a negative radial gradient in the energetic ion pressure profile produces a small increase in the RSAE frequency, such that the results derived from a purely MHD analysis must be compensated for using a value of γ which is increased over that of the 'actual' value. Thus, it may be that some of the residuals in the data are due to an unaccounted for effect of the energetic ions. Future experiments dedicated to the study of RSAEs may be able to provide even tighter constraints on this value with direct measurements of the energetic ion pressure profile. Given the tendency of the energetic ions and the impurities to effectively reduce γ below that derived in their absence it seems reasonable to speculate that the range of γ reported here represents an upper bound.

Acknowledgments

The authors wish to thank the Alcator C-Mod team for supporting these studies. This work was funded by the US DOE under contract numbers DE-FC02-99-ER54512 and DE-FC02-04ER54698.

References

[1] Rosenbluth M N and Rutherford P H 1975 *Phys. Rev. Lett.* **34** 1428
[2] Belcher J W 1987 *Science* **238** 170
[3] Balbus S A and Hawley J F 1991 *Astrophys. J.* **376** 214
[4] Alfvén H 1942 *Nature* **150** 405
[5] Wilson J R *et al* 1993 *Proc. 14th Int. Conf. Plasma Phys. Control. Fusion Research (Wurzburg, Germany)* vol I p 661
[6] Wong K L 1988 *Bull. Am. Phys. Soc.* **33** 209
[7] Wong K L *et al* 1996 *Phys. Rev. Lett.* **76** 2286
[8] Heidbrink W W *et al* 2007 *Phys. Rev. Lett.* **99** 245002
[9] White R B, Gorelenkov N N, Heidbrink W W and Van Zeeland M A 2010 *Plasma Phys. Control. Fusion* **52** 045012
[10] Sharapov S E *et al* 2002 *Phys. Plasmas* **9** 2027
[11] Porkolab M , Rost C, Basse N, Dorris J, Edlund E M, Lin L, Lin Y and Wukitch S J 2006 *IEEE Trans. Plasma Sci.* **34** 229
[12] Van Zeeland M A, Austin M E, Gorelenkov N N, Heidbrink W W, Kramer G J, Makowski M A, McKee G R, Nazikian R, Ruskov E and Turnbull A D 2007 *Phys. Plasmas* **14** 056102
[13] Edlund E M, Porkolab M, Kramer G J, Lin L, Lin Y and Wukitch S J 2009 *Phys. Plasmas* **16** 56106
[14] Sharapov S E *et al* 2006 *Proc. of the 21st IAEA Conf. (Chengdu, China)* vol IAEA-CN-149 (Vienna: International Atomic Energy Agency) p EX/P6-19
[15] Goedbloed J P, Holties H A, Poedts S, Huysmans G T A and Kerner W 1993 *Plasma Phys. Control. Fusion* **35** B277
[16] Li Y M, Mahajan S M and Ross D W 1987 *Phys. Fluids* **30** 1466
[17] Kramer G J, Cheng C Z, Kusama Y, Nazikian R, Takeji S and Tobita K 2001 *Nucl. Fusion* **41** 1135
[18] Berk H, Borba D N, Breizman B N, Pinches S D and Sharapov S E 2001 *Phys. Rev. Lett.* **87** 185002
[19] Breizman B N, Pekker M S and Sharapov S E 2005 *Phys. Plasmas* **12** 112506
[20] Gorelenkov N N, Kramer G J and Nazikian R 2006 *Plasma Phys. Control. Fusion* **48** 1255
[21] Kramer G J, Gorelenkov N N, Nazikian R and Cheng C Z 2004 *Plasma Phys. Control. Fusion* **46** L23
[22] Lipschultz B, Pappas D A, LaBombard B, Rice J E, Smith D and Wukitch S J 2001 *Nucl. Fusion* **41** 585
[23] May M J, Fournier K B, Goetz J A, Terry J L, Pacella D, Finkenthal M, Marmar E S and Goldstein W H 1999 *Plasma Phys. Control. Fusion* **41** 45
[24] Tang V *et al* 2007 *Plasma Phys. Control. Fusion* **49** 873
[25] Hutchinson I H 2002 *Principles of Plasma Diagnostics* 2nd edn (Cambridge: Cambridge University Press) p 371
[26] Porkolab M *et al* 1997 *Proc. of the 1997 EPS Conf. on Controlled Fusion and Plasma Physics* vol 21A p 569
[27] Mazurenko A 2001 Phase contrast imaging on the Alcator C-Mod tokamak *PhD Thesis* Massachusetts Institute of Technology

[28] Snipes J A *et al* 2005 *Phys. Plasmas* **12** 056102
[29] Cheng C Z and Chance M S 1987 *J. Comput. Phys.* **71** 124
[30] Lao L L, St John H, Stambaugh R D, Kellman A G and Pfeiffer W 1985 *Nucl. Fusion* **25** 1611
[31] Edlund E M 2009 A study of reversed shear Alfvén eigenmodes in Alcator C-Mod using phase contrast imaging *PhD Thesis* Massachusetts Institute of Technology
[32] Chu M S, Greene J M, Lao L L, Turnbull A D and Chance M S 1992 *Phys. Fluids* B **4** 371
[33] Winsor N, Johnson J and Dawson J 1968 *Phys. Fluids* **11** 2448
[34] McKee C F and Zweibel E G 1995 *Astrophys. J.* **440** 686
[35] Nazikian R, Kramer G J, Cheng C Z and Gorelenkov N N 2003 *Phys. Rev. Lett.* **91** 125003
[36] Gorelenkov N N 2008 *Phys. Plasmas* **15** 110701
[37] Mazur V A and Mikhajlovskji A B 1977 *Nucl. Fusion* **17** 193